24th INTERNATIONAL CONGRESS ON SOUND AND VIBRATION
23–27 July 2017, London

NUMERICAL INVESTIGATIONS OF MEMBRANE-TYPE ACOUSTIC METAMATERIALS WITH ECCENTRIC MASSES FOR BROADBAND SOUND ISOLATION

Siu-Kit LAU

Department of Architecture, School of Design and Environment, National University of Singapore, Singapore, 117566
email: slau@nus.edu.sg

Zhenbo LU, Kah Hsien LIM, Yiyuan LIU, Boo Cheong KHOO

Temasek Laboratories, National University of Singapore, Singapore, 117411
email: tslluz@nus.edu.sg, brandon.lim@u.nus.edu, tslliuyy@nus.edu.sg, mpekbc@nus.edu.sg

Xiang YU

*Institute of High Performance Computing, A*STAR, Singapore, 138632*
email: yuxiang@ihpc.a-star.edu.sg

Membrane-type acoustic metamaterials (MAMs) which are novel, lightweight and compact materials can be used to screen sound at a particular frequency band. Thus, it opens many possibilities toward producing a new generation of acoustic materials and sensor devices. In the present paper, an efficient scheme of finite element modelling for the acoustic-structural interaction of MAMs with eccentric masses is developed, and this model is used to optimize the eccentric masses' distributions (such as thicknesses, weights, shapes, separations and locations of the masses) for improving acoustic performance. Results show that the optimized eccentric masses' distribution can significantly broaden the frequency range of sound insulation. Furthermore, the membrane-acoustic interactions are explored for better understanding the physical mechanism.

Keywords: Membrane-type acoustic metamaterials (MAMs), eccentric masses, sound insulation, building acoustics, finite element modelling

1. Introduction

The idea of metamaterials with negative properties in an electromagnetic wave was first proposed by Veselago [1]. He postulated a theory of possible materials having negative electric permittivity (ε) and magnetic permeability (μ), thus resulting in a negative refractive index. However, this concept did not attract much research interest until decades ago. Pendry [2] suggested the theoretical possibility of making electromagnetic metamaterials. For electromagnetic waves, negative values of the electric permittivity and magnetic permeability yield many new phenomena, such as negative phase velocity, evanescent waves, and superlensing. Metamaterial antennas have been applied in cellular phone technologies. For instance, the LG Chocolate BL40 mobile handset [3] enables antennas to be sized on the order of one-tenth the signal's wavelength, while still providing a level of performance equal to or better than conventional antennas sized one-half the signal's wavelength, thereby reducing antenna size by a factor of five.

As a counterpart to electromagnetic metamaterials, acoustic metamaterials remain in a stage of infancy. Generally, acoustic metamaterials possess negative mass density and/or negative bulk modulus [4]. Constitutive parameters for wave propagation can be made negative in certain metamaterials using engineered unit cells of sizes smaller than the wavelength, which provides a capability similar to invisibility cloaking, bending waves in the "wrong" direction, and subwavelength imaging. These materials also promise sound insulation and absorption at low frequencies that are dramatically better than conventional systems of similar dimensions and weight. Phononic crystals consisting of solid spheres with relatively high densities and a coating of elastically soft materials have been considered as metamaterials to provide negative mass density for sound insulation [5]. Yang et al. [6] proposed a membrane-type acoustic metamaterial (MAM) that allows for a thinner structure. MAM is formed by an elastic membrane fixed by a rigid frame, with a small weight at the centre of the membrane for tuning the resonances. With a thickness of less than 15 mm and weight less than 3 kg/m^2, this MAM panel reveals 20 dB of sound transmission loss at around 200 Hz. The eccentricity of attached mass and ring masses were studied for wider broadband sound isolation [7-8].

In order to explore the optimized design of sound isolation and absorption materials using MAM, an efficient scheme of finite element modelling for the acoustic-structural interaction of MAM with eccentric masses is developed. This model is used to optimize the eccentric masses' distributions (such as thicknesses, weights, shapes, separations and locations of the masses) for achieving better acoustic performance.

2. Simulation configurations

The schematic of the simulation configuration for the MAM is shown in Fig. 1. It is a duct with a cross-section of $160mm \times 160mm$. A MAM comprising of the 'Membrane' and 'Mass(es)' is support by a frame that firmly installed at the middle position of the duct. The plane wave sound source is introduced at 'Transmitting plane' and then propagating along the duct. Non-reflection condition [i.e. Perfectly Matched Layer (PML)] is applied on the 'Receiving plane' to guarantee the sound wave can only propagate one direction through this plane without any reflection. The transmission losses (TL) for the MAM is calculated using the sound energy comparison between the 'Receiving plane' and 'Transmitting plane'.

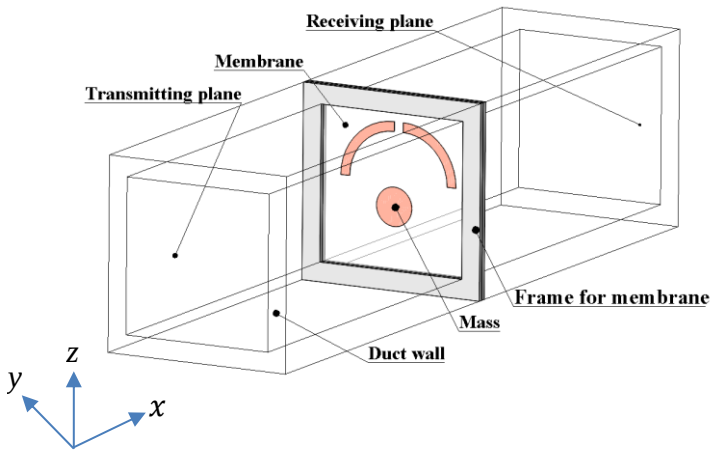

Figure 1: Schematic of the simulation configuration for the MAM

This MAM model is built in the COMSOL commercial multi-physics software using the finite element method for studying its acoustic performance. A radially pre-stretched dielectric elastomer (DE) film (3M VHB 4910, the original thickness is 1.0mm) was used for the present paper, this material was used in the previous research work for the tunable acoustic absorber [9-13]. Assuming that the original radius of the DE film is r_0, it can be stretched to the new radius r, thus the pre-stretch ratio is $\lambda = \frac{r}{r_0}$, and the thickness of pre-stretched membrane is $t = \frac{1}{\lambda^2}$. The DE membrane used in the validation is stretched to a ratio 1.77 and the tension is experimentally identified as 26.11N/m.

The thickness, density and the Young's module for the pre-stretched membrane are 0.319mm, 1009.2kg/m^3, and 0.22MPa respectively. DE membrane is a hyper-elastic material, therefore, several hyper-elastic models are used for the present validation, including Mooney-Rivlin [14-15] and Yeoh [16] hyper-elastic model. The material parameters of the two models are shown in Table 1. The comparison results are shown in Fig. 2. Experiments was carried out with the same setup in Fig. 1 with two-load source method [17]. The results of the numerical models are agree with that measured in the experiment. It also was concluded from the existing publication that the Yeoh hyper-elastic model is the more suitable model for the DE membrane [18]. Therefore, the Yeoh's hyper-elastic model is applied as the simulation model for the present paper.

Table 1: Material parameters for the Yeoh and the Mooney-Rivlin hyper elastic model [18]

Yeoh		
C_{10}	[MPa]	0.0693
C_{20}	[MPa]	-8.88 x 10^{-4}
C_{30}	[MPa]	16.7 x 10^{-6}
Mooney-Rivlin		
C_{10}	[MPa]	0.0450
C_{01}	[MPa]	0.0412

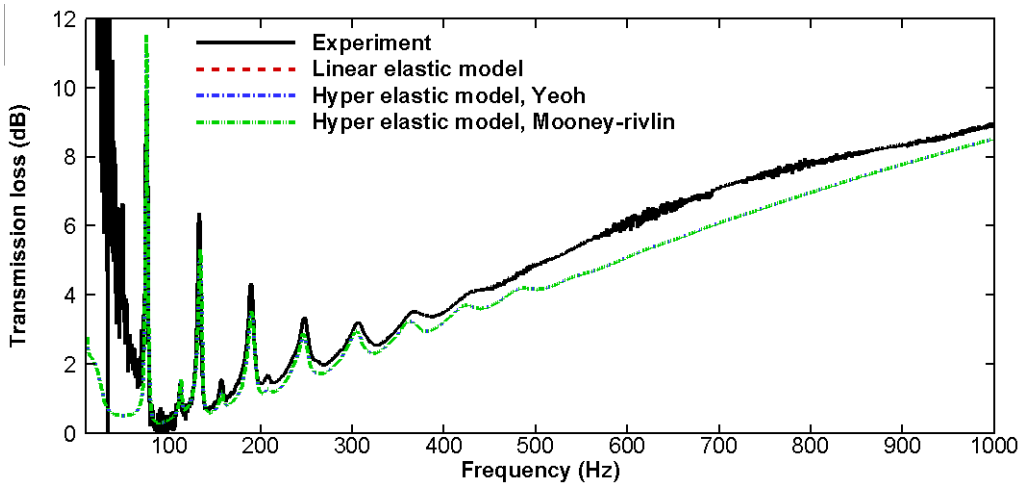

Figure 2: Validation of the numerical model using various elastic model with experimental results

3. Results and discussions

One of the advantages of the hyper-elastic material 1.0mm-thickness VHB 4910 is that it can be stretched to different ratios λ with a uniform distribution inner stress, and this stress can be experimentally identified. Table 2 shows the parameters of different radially pre-stretch DE membranes.

The transmission loss of the DE membranes with various pre-stretch ratios λ are calculated using the developed FEM numerical model and results are shown in Fig. 3. As shown in Fig. 3, the main resonance peaks are distributed in the frequency range of 50Hz to 300Hz, and they can be shifted to high frequency range due to the increase inner stress which is caused by the increment of the pre-stretch ratio λ, and the amplitudes of these peaks are almost kept at the same values. However, the thickness of the membrane is decrease as the second power of pre-stretch ratio λ, therefore, the TLs of the membranes for the higher pre-stretch ratio λ at the frequency range 300Hz to 1000Hz are worse than that of the lower pre-stretch ratio λ. Of course, thicker membrane has the heavier weight which should be important issue to be considered.

If the membranes are kept at the same pre-stretch ratio, say $\lambda = 1.77$, but the thickness of the membranes are increased from 0.319mm to 0.638mm and 0.957mm, by doing this way, the tension on the membrane can be increased. The results are plotted in the Fig. 4. It is found in Fig. 4 that the

resonance peaks are kept the same for different thickness, but the TL values from 100Hz to 1000Hz are increased as the increment of the membrane's thickness.

Table 2: Parameters of different radially pre-stretched membranes

Pre-stretch ratio λ	Thickness t (mm)	Tension T_0 (N/m)
2	0.25	21.82
3	0.11	21.51
4	0.0625	20.17
5	0.04	18.99

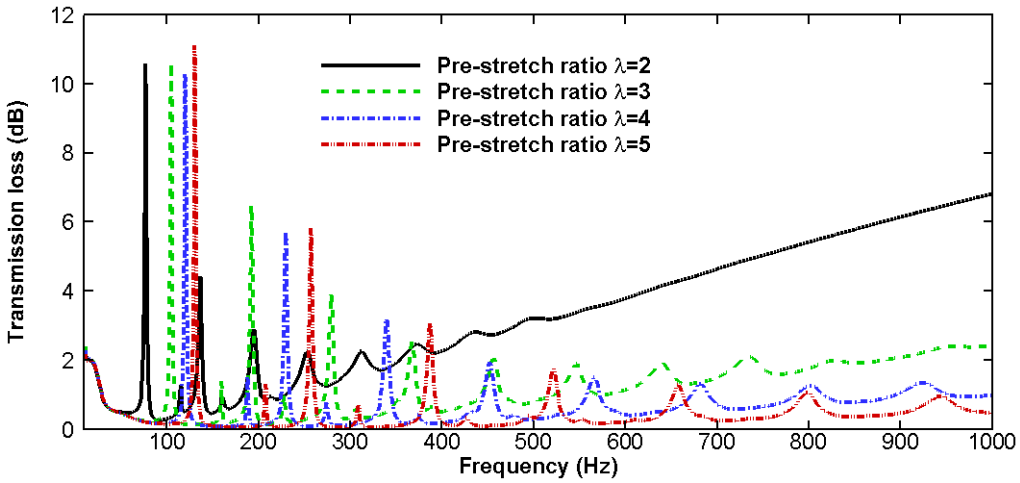

Figure 3: Transmission loss for different pre-stretched membranes.

Therefore, the resonance peaks are mainly due to the inner stress of the membrane. By only increasing the pre-stretch ratios or thickness of the membrane, it cannot contribute to any low-frequency range increment in the attenuation band of 50-300Hz. In addition, the weight of the 0.957mm thick membrane is 24.72g as compared to the 0.319mm thick counterpart's 8.24g. Thus, a compromise between the weight and TL should be reached when considering acoustic performance at higher frequency (>200Hz).

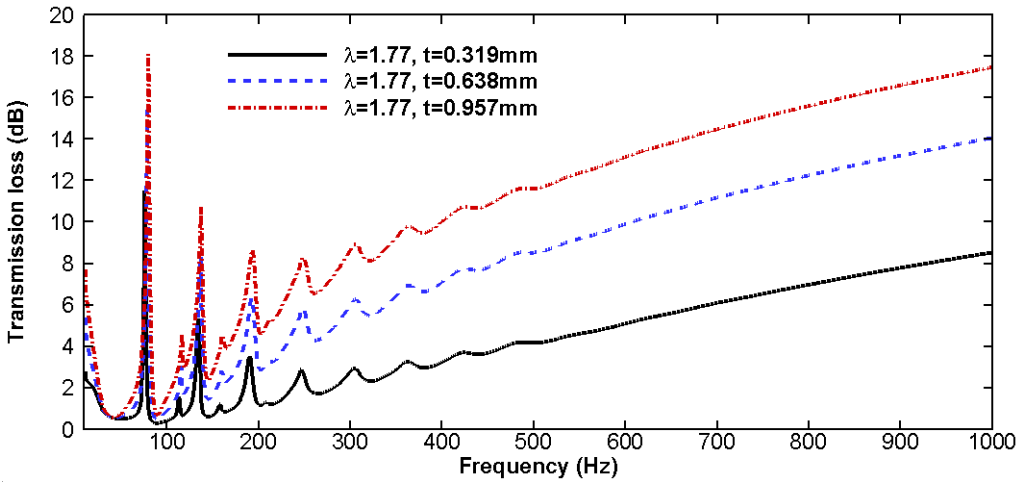

Figure 4: Transmission loss for various membranes' thickness t.

In order to improve the acoustic performance of MAM in the low-frequency range, various mass configurations are used, as listed in Fig. 5. They are: (1) Center point mass with a radius $R_0 = 6mm$; (2) Ring mass with different outer R_2 and inner radius R_1; (3) Split ring mass with outer radius $R_4 =$

$50mm$ and inner radius $R_3 = 40mm$, the space between each split part is $d = 20mm$. All these masses are cut from a 0.4mm-thickness aluminium plate. The mass added on the membrane can induce new resonance peaks, and the larger radius mass can constraint some vibration modes of the membrane that can change the resonance peaks. Furthermore, spaces between the split ring masses might allow the membrane and part of the mass vibrate independently for the possible new resonance peaks. Of course, the different combinations can have various acoustic performance, so it is very complex to consider all these possibilities. In the present paper, the configurations shown in Fig. 5 are considered. The knowledge obtained from these configurations can benefit the optimized mass distribution design.

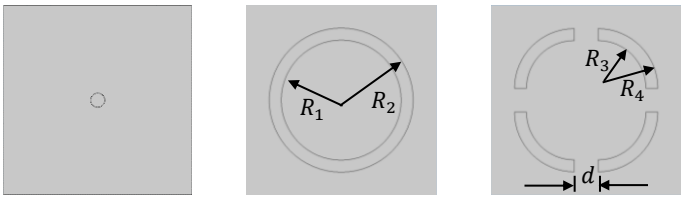

Figure 5: Various mass configurations on the membrane. From left to right: (1) Center point mass with a radius 6mm; (2) Ring mass with different outer and inner radius; (3) Split ring mass with outer radius 50mm and inner radius 40mm. All these masses are cut from 0.4mm aluminium plate.

Adding the mass configurations as shown in Fig. 5 on the DE membrane, the TL is calculated using the developed numerical FEM model and the results are shown in Fig. 6. It can be observed that the first peak locates at 76.23Hz for the membrane, and the band for 5dB-TL is from 73.94Hz to 77.65Hz, a very narrow band of 3.71Hz. A 6mm-center-point-mass can shift the first peak to a lower frequency 69.95Hz, but the 5dB-TL band is the same as the membrane. The circular ring mass can induce new peaks which locate at 73.66Hz, 86.21Hz and 91.92Hz, and the 5dB-TL band is significantly increased to 14.54Hz (a increment of 391%). The split ring mass configuration can shift the peak to the location 109.96Hz, and the 5dB-TL band is 13.12Hz (an increment of 353%) which is similar to the resultant bandwidth of the circular ring mass and still quite significant when compare with the results of membrane. Thus, the masses added on the membrane can shift and the resonance peaks of the membrane, and at some of the configuration, say circular ring mass and split ring mass, it can significantly increase the attenuation band of 5dB-TL.

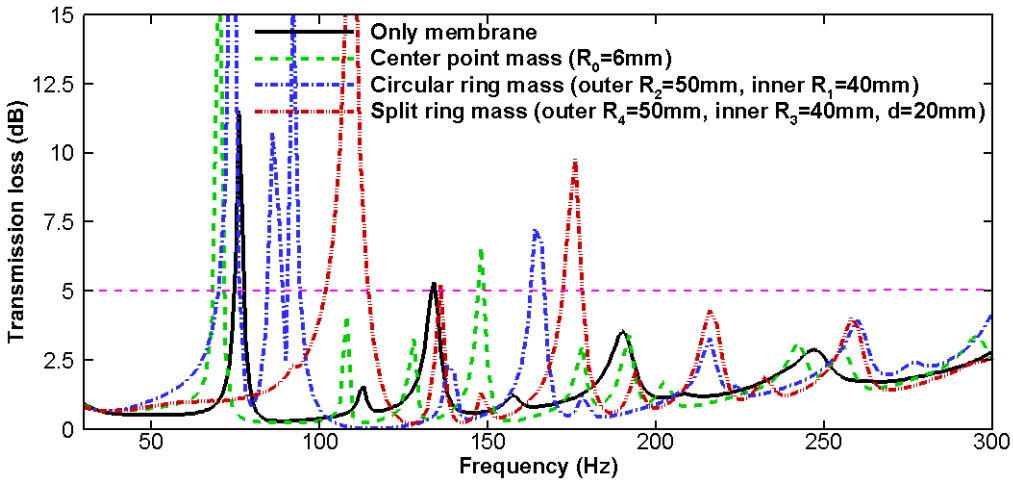

Figure 6: Comparison of various mass distributions.

There are several parameters can affect the acoustic performance of the MAM, such as the density of the materials and the radius of the circular ring mass. In the following section, the effect of the radius is explored. As shown in Fig. 7, a smaller radius, say outer radius 30mm and inner radius 20mm, the acoustic performance is quite similar to the results of the center point mass. By increasing the radius, more peaks appear, and these peaks are shifted to different locations. At the case of outer

radius 50mm and inner radius 40mm, the peaks are close enough to generate a new widest band that is found in both Fig. 5 and 6. Further increase the radiuses; the peaks combination will be continuously changed. Thus by changing the radius of the circular ring mass, the acoustic performance will be enhanced if the new generated peaks can come close to each other for forming a new wider band.

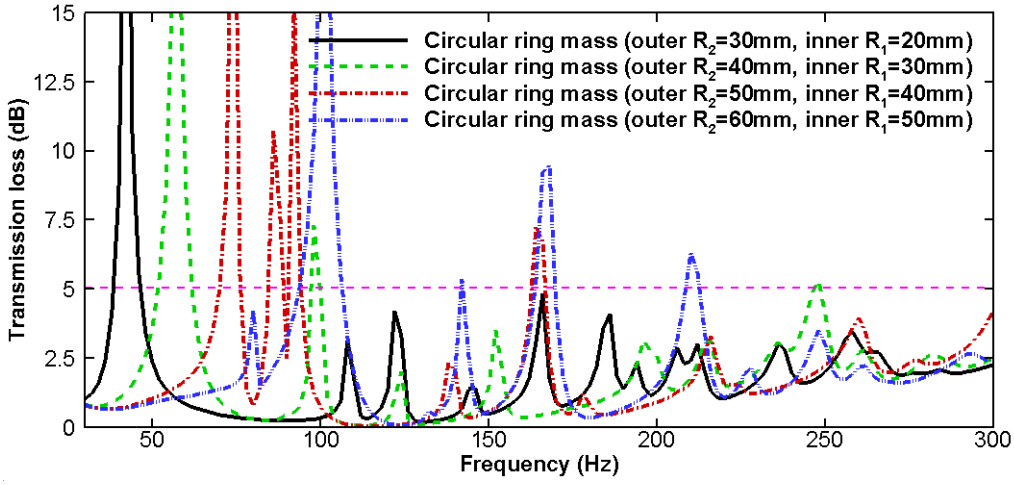

Figure 7: Comparison of circular ring masses with various outer and inner radiuses.

To be concluded, the developed FEM numerical model was used to study the optimized mass and membrane distribution on the MAM. It is found that at high frequency, say 200Hz to 1000Hz, thicker membrane has better acoustic performance, which follows the mass-law. While in the lower frequency range, say 40Hz to 300Hz, the resonance peaks can only be changed by using various mass configurations. The best mass configurations for the present paper is the circular ring mass with outer radius 50mm and inner radius 40mm, which can significantly increase the 5dB-TL band to 391% when comparing with that of the membrane.

4. Conclusions

An efficient scheme of finite element modelling for acoustic-structural interaction of MAM with eccentric masses was developed in the present paper, this model was validated using the experimental data. The acoustic performance of the MAM can be optimized by seeking the optimization of the eccentric masses' distributions, such as thicknesses, weights, shapes, separations and locations of the masses. The best mass configurations for the present paper is the circular ring mass with outer radius 50mm and inner radius 40mm, it can significantly increase the 5dB-TL band when comparing with that of the membrane.

For future study, more research work will done for understanding the optimization strategy and experimental work will be conducted to validate the optimized mass configuration.

REFERENCES

1 Veselago, Viktor G. 1968. "The electrodynamics of substances with simultaneously negative values of ε and μ." *Soviet Physics Uspekhi* 10 (4):509-514.
2 Pendry, J. B. 2000. "Negative Refraction Makes a Perfect Lens." *Physical Review Letters* 85 (18):3966-3969.
3 Das, Saswato R. 2009. Metamaterials arrive in cellphones. *IEEE Spectrum* 2016 (28 October). Accessed 2 April 2016.
4 Ding, Yiqun, Zhengyou Liu, Chunyin Qiu, and Jing Shi. 2007. "Metamaterial with simultaneously negative bulk modulus and mass density." *Physical review letters* 99 (9):093904.
5 Wester, Eric, Xavier Brémaud, and Bryan Smith. 2009. "Meta-material sound insulation." *Building Acoustics* 16 (1):21-30.

6 Yang, Z., H. M. Dai, N. H. Chan, G. C. Ma, and Ping Sheng. 2010. "Acoustic metamaterial panels for sound attenuation in the 50–1000 Hz regime." *Applied Physics Letters* 96 (4):041906.

7 Chen, Yangyang, Guoliang Huang, Xiaoming Zhou, Gengkai Hu, and Chin-Teh Sun. 2014. "Analytical coupled vibroacoustic modeling of membrane-type acoustic metamaterials: Membrane model." *The Journal of the Acoustical Society of America* 136 (3):969-979.

8 Naify, Christina, Chia-Ming Chang, Steven Nutt, and Geoffrey McKnight. 2011. "Transmission loss of membrane-type acoustic metamaterials with coaxial ring masses." *Journal of Applied Physics* 110 (12):124903-124903-8.

9 Z. Lu, Y. Cui, M. Debiasi and Z. Zhao, A Tunable Dielectric Elastomer Acoustic Absorber, Acta Acustica united with Acustica, 101 (2015) 863-866.

10 Z. Lu, H. Godaba, Y. Cui, C.C. Foo, M. Debiasi and J. Zhu, An electronically tunable duct silencer using dielectric elastomer actuators, The Journal of the Acoustical Society of America, 138 (2015) EL236-EL241.

11 Z. Lu, Y. Cui and M. Debiasi, Active membrane-based silencer and its acoustic characteristics, Applied Acoustics, Volume 111, 2016, Pages 39–48.

12 X. Yu, Z. Lu, L. Cheng and F. Cui, Vibroacoustic modeling of an acoustic resonator tuned by dielectric elastomer membrane with voltage control, Journal of Sound and Vibration, Volume 387, 20 January 2017, Pages 114–126.

13 X. Yu, Z. Lu, F. Cui, L. Cheng and Y. Cui, Tunable acoustic metamaterial with an array of resonators actuated by dielectric elastomer, Extreme Mechanics Letters, Volume 12, April 2017, Pages 37–40.

14 Mooney. M., (1940) *A theory of large elastic deformation*. Journal of Applied Physics 11 (9), 582–592.

15 Rivlin, R.S., (1948) *Large elastic deformations of isotropic materials. IV. Further developments of the general theory*. Philosophical Transactions of the Royal Society. A 241 (835), 379–397.

16 Yeoh, O.H., (1993) *Some forms of the strain energy function for rubber*. Rubber Chem-istry and Technology 66, 754–771

17 T.Y. Lung and A. G. Doige, "A time-averaging transient testing method for acoustic properties of piping systems and mufflers with flow," *J. Acoust. Soc. Am*, 73, pp. 867-876, 1983.

18 Michael Wisslera, Edoardo Mazzab, Modeling of a pre-strained circular actuator made of dielectric elastomers, Sensors and Actuators A: Physical, Volume 120, Issue 1, 29 April 2005, pp. 184-192.